MIMO-RSFT Radar: A Reduced Complexity MIMO Radar Based on the Sparse Fourier Transform

Shaogang Wang, Vishal M. Patel and Athina Petropulu
Department of Electrical and Computer Engineering
Rutgers, the State University of New Jersey, Piscataway, NJ 08854, USA
Email: {shaogang.wang, vishal.m.patel, athinap}@rutgers.edu

***Abstract*—Despite their advantages, MIMO radars have not seen a massive deployment. One of the main limitations of the MIMO radar is its implementation cost, stemming from the large number of transmit and receive radio frequency channels, and the high data throughput that results in costly digital signal processing (DSP). This paper proposes MIMO-RSFT radar, a MIMO radar which employs the Realistic Sparse Fourier transform (RSFT) and achieves reduced DSP complexity. Slow-time and fast-time coded waveforms are investigated in the context of the MIMO-RSFT radar. The key steps of deriving the optimal detection thresholds for the MIMO-RSFT radar in 3-D are provided, and the feasibility of the MIMO-RSFT radar is demonstrated via simulations.**

***Index Terms*—Array signal processing, sparse Fourier transform, MIMO radar.**

I. Introduction

A collocated multi-input multi-output (MIMO) radar [1], [2] can see targets everywhere at anytime without steering its beams as a traditional phased array radar does. The MIMO radar's wide angle coverage is achieved by multiple channels for transmitting and receiving. During the transmission, a set of mutually orthogonal waveforms are transmitted by each array element with an omni-directional beam pattern; after the signal is received from each digitized receiving channel, multiple narrow beams are formed in the digital signal processor (DSP) using beamforming methods. A typical MIMO radar structure is shown in Fig. 1 with an uniform linear array (ULA) configuration. Although MIMO radars enjoy improved parameter identifiability and larger number of targets that can be simultaneously identified compared to its phased array counterpart [2], they have not been widely used in practical applications. One of the reasons is the high implementation cost involved, which is mainly due to: 1) the large number of transmit and receive radio frequency (RF) channels; and 2) the high data throughput and complex processing, which results in costly DSPs. The cost of the RF channels can be reduced by sharing the transmit and receive antennas, i.e., each antenna element can be used both for transmitting and receiving in a *pulse mode* [1]. In this paper, we will assume such configuration and address the reduction of the cost of DSP.

Modern pulse radars usually employ the pulse compression (PC) technique to increase their sensitivity (ability to detect weak signals) and range resolution. To implement PC in MIMO radars, the waveforms must have good cross- and auto-correlation properties [3], which are properties needed for PC and *waveform decoding* (WD). WD is a process that separates the orthogonal waveforms from each transmitter, so that the so called *transmit beamforming* [1] can be applied subsequently to compensate for time delay caused during transmission. To this end, code division multiple access (CDMA) waveforms [3], [4] are usually adopted. Depending on the application, the baseband CDMA code sequences can be applied on the slow-time (time across pulses) or on the fast-time (time within a single pulse), yielding different processing schemes and computational complexities (see Section III).

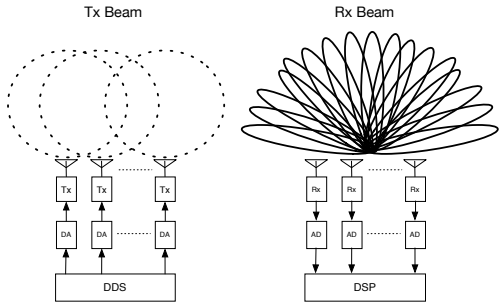

Fig. 1. **Collocated MIMO Radar System with ULA.** The half-wavelength spacing ULA with N elements is used both for transmitting and receiving. Each element transmits an orthogonal waveform, which is generated by a direct digital synthesizer (DDS). The orthogonality of the waveforms results into an omni-directional transmit beam pattern, while multiple narrow beams are formed simultaneously by the beamforming in the DSP.

The high degrees of freedom in MIMO radars results in high dimensional computations. For the MIMO radar of Fig. 1, in order to detect targets and estimate their range and direction-of-arrival (DOA), we need to do processing in a 3-D space, i.e., range, transmit DOA and receive DOA. Although parametric methods yield in general better resolution, conventional, Fourier transform-based methods are often preferable in practice due to their robustness to noise and their lower computational complexity [5]. In fact, matched filtering for range processing, and transmit and receive beamforming for DOA processing can be effectively implemented via the fast Fourier transform (FFT) (see e.g., [6]), which (see Fig. 3) has a complexity of $O(RN^2 \log(RN^2))$ for each pulse repetition interval (PRI), where N, R are the number of array elements and the number of the range bins, respectively. When N, R are large, or, when the dimension of signal processing continuous

to increase (for instance, when both azimuth and elevation DOA are considered), the computation of the FFT becomes costly.

The recently introduced Sparse Fourier transform (SFT) [7], leverages the sparsity of signals in the frequency domain and achieves substantial reduction of the complexity required to identify the underlying frequencies. In the radar scenario, the number of targets within the radar coverage is usually far less than the number of resolution cells in the high dimensional parameter space, which motivates the application of SFT in radar processing. However, most of the existing SFT algorithms require that the signal frequencies to be on the grid and the exact sparsity to be known. In our previous work [8], [9], we proposed the Realistic Sparse Fourier Transform (RSFT) algorithm, which introduces a *pre-permutation windowing* to address the off-grid frequencies and employs Neyman-Pearson (NP) detection to identify frequencies without knowledge of the exact sparsity.

In this paper, by leveraging our prior work [8], [9] we make the following contributions:

1) We propose MIMO-RSFT radar, a reduced complexity MIMO radar that employs the RSFT to reduce the cost of the DSP.
2) We explore slow-time and fast-time coded waveforms that support PC for MIMO radars. The implementation of the RSFT and the resulting computational savings are investigated for both cases.
3) We provide the key steps of deriving the optimal detection thresholds for the MIMO-RSFT radar based on the signal model.

In our previous work [8], [9], an example of employing the RSFT at the ubiquitous radar [10] was presented. The ubiquitous radar has one transmitting channel and multiple receiving channels, so it can be viewed as a single-input multi-output (SIMO) radar. Compared to the SIMO radar scenario, implementing the RSFT on a MIMO radar is more involved, as in this case, the signal is not naturally sparse in the range dimension. Moreover, additional processing needs to be done, i.e., WD, PC and transmit beamforming. Extending our previous work, we provide the key steps of deriving the optimal detection thresholds in high dimensions, and make some connections between the 1-D and N-D cases. Sparse sensing in MIMO radars has received significant attention, with compressed sensing-based MIMO (MIMO-CS) radar [11] and matrix completion-based MIMO (MIMO-MC) radar [12], being two recent approaches. Compared to MIMO-CS and MIMO-MC radars, which reduce sample complexity of the signal processing, the MIMO-RSFT radar aims at decreasing computational complexity, which would allow for more affordable hardware in real time processing.

Notation: We use lower-case (upper-case) bold letters to denote vectors (matrices). $(\cdot)^T$ and $(\cdot)^H$ respectively denote the transpose and conjugate transpose of a matrix or a vector, while $(\cdot)^*$ is the conjugate of a scalar. $\|\cdot\|$ is the Euclidean norm for a vector. We use $*$ to denote the convolution of two vectors. $[\mathbf{a}]_i$ is the i_{th} element of vector $\mathbf{a}$, while $[\mathbf{A}]_{u,v,w}$ is the $(u,v,w)_{\text{th}}$ element of tensor $\mathbf{A}$. $[S]$ refers to the set of indices $\{0,...,S-1\}$, and $[S]\setminus a$ is for eliminating element a from set $[S]$. We use $\text{diag}(\cdot)$ to denote forming a diagonal matrix from a vector. The DFT of signal $\mathbf{s}$ is denoted as $\hat{\mathbf{s}}$. We also assume that the signal length in each dimension is an integer power of 2.

II. Signal Model and Problem Formulation

We consider the MIMO radar configuration of Fig. 1. During transmission, a set of orthogonal CDMA waveforms are transmitted by each antenna element. Let us denote the discrete baseband signal, which is transmitted by the $u_{\text{th}}, u \in [N]$ element in the $s_{\text{th}}, s \in [T]$ PRI by $\mathbf{s}_{u,s} \in \mathbb{C}^M$. Suppose that there are K targets within the radar coverage. For simplicity, we do not incorporate Doppler in our signal model, thus implicitly assuming that the targets are moving slowly and their Doppler can be neglected. Note that including the Doppler processing in the MIMO-RSFT radar is straightforward, and is briefly discussed in Section IV-D. The received signal of the $i_{\text{th}}, i \in [N]$ receiving channel (after quadrature demodulation and analog to digital conversion) is $\mathbf{r}_{i,s} \in \mathbb{C}^R$, which is a superposition of the signals that are returned from K targets, i.e.,

$$\mathbf{r}_{i,s} = \sum_{k\in[K]} \left(b_{k,s} e^{ji\pi \sin\theta_k} \sum_{u\in[N]} \mathbf{a}_{u,s}(t_k) e^{ju\pi \sin\theta_k} \right) + \mathbf{n}_s, \tag{1}$$

where $t_k \in [R-M], \theta_k \in [-\pi/2, \pi/2]$ denote sample delay and DOA (the angle between the line-of-sight of target and the array normal) of the k_{th} target, which are unknown deterministic quantities and are assumed to be stationary within T PRIs. The phase terms $e^{ji\pi \sin\theta_k}$ and $e^{ju\pi \sin\theta_k}$ are respectively caused by the channel-wise time delay during reception and transmission, by assuming that the signal is narrow-band and the array elements are spaced apart by half wavelength. We use $\mathbf{a}_{u,s}(t_k) \in \mathbb{C}^R, R > M$ to represent the fast-time data samples within the s_{th} PRI, which contains a delayed by t_k version of $\mathbf{s}_{u,s}$, i.e., $[\mathbf{a}_{u,s}]_{v+t_k} = [\mathbf{s}_{u,s}]_v, v \in [M]$, and the other entries of $\mathbf{a}_{u,s}$ equals to zero. The $b_{k,s}$ is the complex amplitude of the k_{th} target, which is circularly symmetric Gaussian and distributed as $b_{k,s} \sim \mathcal{CN}(0, \sigma_{bk}^2)$; the noise $\mathbf{n}_s$ is temporal and spatial white, distributed as $\mathbf{n}_s \sim \mathcal{CN}(\mathbf{0}, \sigma_n^2 \mathbf{I})$, where $\mathbf{0}$ is R-dimensional zero vector, and $\mathbf{I} \in \mathbb{R}^{R\times R}$ is the identity matrix.

Let $\mathbf{R}_s = [\mathbf{r}_{0,s}, \ \mathbf{r}_{1,s}, \ \cdots \ \mathbf{r}_{N-1,s}]$ represent the data collected by all antennas. The data collected over T pulses, i.e., $\mathbf{R}_s, s \in [T]$, will be used to detect the targets and estimate their range and DOA. The conventional processing schemes for slow-time and fast-time coded waveforms are presented in Fig. 2 (a) and Fig. 3 (a), where WD and PC are implemented sequentially and simultaneously, respectively. Conceptually, WD separates each $\mathbf{a}_{u,s}(t_k)e^{ju\pi \sin\theta_k}$ component in $\mathbf{r}_{i,s}$, while PC convolves $\mathbf{a}_{u,s}(t_k)$ with $\mathbf{s}_{u,s}$ to achieve high range resolution. After that, the transmit and receive beamforming are implemented along the transmit and receive channel,

respectively. Subsequently, after a non-coherent accumulation, a detection procedure on each resolution cell is applied.

The FFT and inverse FFT (IFFT) can be employed in various stages of the processing, however, the complexity is still high due to high dimensional data. In what follows, we explain how one can use the RSFT in both slow-time and fast-time coding schemes to save computation.

III. Slow-time and Fast-time Coded Waveforms Processing

Let us consider the transmit waveforms to be unimodal [3], i.e., $|[\mathbf{s}_{u,s}]_i| = 1, i \in [M]$. First, we discuss the orthogonality and PC requirements for such waveforms. Based on that, we compare the processing schemes for slow-time and fast-time coded waveforms and derive their computational complexities.

The correlation between $\mathbf{s}_{u,s}$ and $\mathbf{s}_{v,s}$ at lag $n, n \in [M]$ equals to $c_{u,v,s}(n) = c^*_{v,u,s}(-n) = \sum_{i=n+1}^{M} [\mathbf{s}_{u,s}]_i [\mathbf{s}_{v,s}]^*_{i-n}$. The slow-time orthogonality requires that the pulses emitted from different transmitters be uncorrelated within L consecutive PRIs, i.e.,

$$\sum_{s\in[L]} c_{u,v,s}(0) = 0,\ u, v \in [N], u \neq v, \tag{2}$$

while the fast-time orthogonality requires that $L = 1$ in (2). Note that (2) guarantees that: 1) the transmit beam-pattern is omni-directional within L PRIs; and 2) the WD can be applied upon reception.

PC requires the auto-correlation of each pulse at different non-zero lags be below certain level, i.e., $|c_{u,u,s}(n)| < \epsilon, n \in [M] \setminus 0$, where $0 \leq \epsilon << |c_{u,u,s}(0)| = M$.

A. Slow-time Coding

The slow-time coding scheme [4] can employ any pulse waveform $\mathbf{s}$ that supports PC (e.g., the Barker code waveform) as its base waveform. To achieve (2), the antennas transmit T/L *bursts*, assuming that T is divisible by L; a burst is composed of L consecutive pulses, i.e., $\mathbf{s}_{u,s}, u \in [N], s \in [L]$, whose initial phases are coded by N mutually orthogonal unimodal sequences (e.g., the Hadamard sequences), which is denoted as $\mathbf{h}_u \in \mathbb{C}^L, u \in [N]$. Hence $\mathbf{s}_{u,s} = [\mathbf{h}_u]_s \mathbf{s}$. Upon reception, WD is applied for each receiving channel on the burst basis by correlating $\mathbf{r}_{i,s}, s \in [L]$ with $\mathbf{h}_u$, yielding $\mathbf{w}_{i,u} \in \mathbb{C}^R, u \in [N]$, i.e.,

$$\begin{aligned}\mathbf{w}_{i,u} &= [\mathbf{r}_{i,0}\ \ \mathbf{r}_{i,1} \cdots \mathbf{r}_{i,L-1}]\mathbf{h}_u \\ &= L \sum_{k\in[K]} b_k e^{j(i+u)\pi \sin\theta_k} \mathbf{a}(t_k) + \tilde{\mathbf{n}},\end{aligned} \tag{3}$$

where $\mathbf{a}(t_k)$ is t_k-delayed version of $\mathbf{s}$; $\tilde{\mathbf{n}}$ is the noise part. The WD process for each burst has a complexity of $O(N^2LR)$. Subsequently, PC is applied by matched filtering $\mathbf{w}_{i,u}$ with $\mathbf{s}$. With the matched filtering being implemented in the frequency domain for efficiency, PC for each burst has a complexity of $O(N^2R\log R)$. The subsequent transmit and receive beamforming for each burst, when implemented with FFT, has a complexity of $O(RN^2 \log N^2)$. Therefore, the complexity of processing each burst is $O(UL + U\log U)$, where $U = RN^2$. Clearly, for T PRIs (T/L bursts), the processing scheme in Fig. 2 (a) gives a complexity of $O(T(U + \frac{U}{L}\log U) + U)$.

B. Fast-time Coding

As opposed to slow-time coding that applies orthogonal coding on the inter-pulse basis, the fast-time coding implements the coding on the intra-pulse basis. However, since the ideal cross- and auto-correlation properties cannot be achieved at the same time [3], the orthogonality and the non-zero lag cross-correlation for the fast-time coded waveforms are approximate, i.e., $|c_{u,v,s}(n)| < \gamma << M$ for $n \in [M], u \neq v$. Upon reception, WD and PC can be simultaneously achieved by matched filtering $\mathbf{r}_{i,s}$ with $\mathbf{s}_{u,s}, u \in [N]$, which yields

$$\begin{aligned}\mathbf{y}_{i,u} &= \mathbf{s}_{u,s} * \mathbf{r}_{i,s} \\ &\approx \sum_{k\in[K]} b_k e^{j(i+u)\pi \sin\theta_k} (\mathbf{s}_{u,s} * \mathbf{a}_{u,s}(t_k)) + \bar{\mathbf{n}},\end{aligned} \tag{4}$$

where $\bar{\mathbf{n}}$ is the noise component. When the matched filtering is implemented in the frequency domain (see Fig. 3 (b)), the complexity is $O(U \log R)$. The subsequent transmit and receive beamforming has a complexity of $O(U \log N^2)$, therefore, the complexity of fast-time coding processing for T PRIs (Fig. 3 (a)) is $O(T(U \log U) + U)$.

IV. RSFT based MIMO Radar Signal Processing

A. The RSFT Algorithm

We briefly summarize the RSFT algorithm in the following. First, a pre-permutation windowing is applied to the data to confine leakage from off-grid frequencies. Then, the *permutation* procedure reorders the input data in the time domain, causing the frequencies to also reorder. The permutation causes closely spaced frequencies to appear in well separated locations with high probability. Then, a frequency-domain *flat-window* [7] is applied on the permuted signal for the purpose of extending a single frequency into a (nearly) boxcar, for a reason that will become apparent in the following. The windowed data are aliased, and the frequency domain equivalent of this *aliasing* is undersampling by U/V, where U, V denote for the original and aliased data length, respectively. The flat-window used at the previous step ensures that no peaks are lost due to the effective undersampling in the frequency domain. After this stage, a FFT of length V is employed. The permutation and the aliasing procedure effectively map the signal frequencies from U-dimensional space into a reduced V-dimensional space, where the *first stage detection* procedure locates the significant frequencies, and then the corresponding indices are *reverse mapped* into the original U-dimensional frequency space. However, the reverse mapping yields not only the true location of the significant frequencies, but also U/V ambiguous locations for each frequency. To remove the ambiguity, multiple iterations of processing with randomized permutation are performed. Finally, the *second stage detection* procedure locates the significant frequencies from the accumulated data for each iteration. The NP criterion are used for both stages of detection. For detailed explanation of the algorithm please refer to [9].

B. RSFT-based MIMO Radar

The conventional processing for slow-time and fast-time coding schemes (see Fig. 2 (a) and Fig. 3 (a)) share a

similar structure, except that their WD and PC processing are different. By packing some of the operations in WD and PC into a so called *range pre-processing* procedure, we are able to present a uniform RSFT-based processing structure for both coding schemes as shown in Fig. 4, which simplifies our discussion on MIMO-RSFT radar for both coding schemes.

1) Range pre-processing: For slow-time coded waveforms, the range pre-processing includes WD and the front-end of PC, which contains the FFTs on the decoded waveform $\mathbf{w}_{i,u}$ and the multiplications between $\hat{\mathbf{w}}_{i,u}$ and $\hat{\mathbf{a}}^*$, as shown in Fig. 2 (b). For fast-time coded waveforms, the range pre-preprocessing contains the front-end of the frequency domain implementation of matched filtering, i.e., the FFTs on $\mathbf{r}_{i,s}$ and the multiplications between $\hat{\mathbf{r}}_{i,s}$ and $\hat{\mathbf{a}}^*_{u,s}$, as shown in Fig. 3 (b).

2) An uniform processing structure for MIMO-RSFT radar: Since the baseband signal is not sparse in the time domain nor in the frequency domain, the RSFT cannot be directly applied on the range domain. However, after PC, the signal becomes sparse in the time domain, which suggests that the backend of PC, i.e., the IFFT can be replaced by the RSFT. Moreover, since the signal is sparse in the DOA domain, both transmit and receive beamforming can be implemented with the RSFT. Hence, after the range pre-processing, we apply a 3-D RSFT on the signal to implement the detection and estimation. The processing scheme for the MIMO-RSFT radar is shown in Fig. 4. Note that, since we summarize the difference of the slow-time and fast-time coding processing in the range pre-processing, the processing structure of Fig. 4 can be applied to both coding schemes.

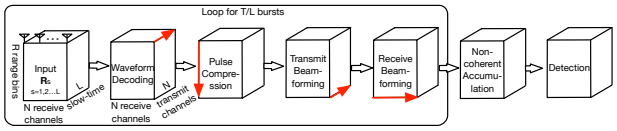

(a)

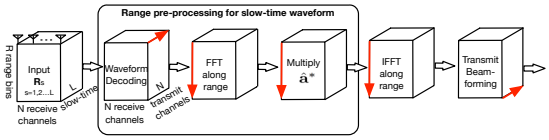

(b)

Fig. 2. **Conventional MIMO Radar Signal Processing for Slow-time Coded Waveforms.** The red arrows indicate the dimension of related processing. (a) Overview of MIMO radar processing for slow-time coded waveforms. WD, PC, transmit and receive beamforming are processed on the burst basis. For better detection performance, a non-coherent accumulation over T/L bursts is applied. (b) Range pre-processing for slow-time coded waveforms.

3) Complexity analysis for MIMO-RSFT radar: As discussed in [9], the complexity of the RSFT is $O(T\phi + U)$, where $\phi = U + V + V\log V + \frac{K\eta_m U}{\eta_p V}$, and η_m, η_p are the pre-permutation window parameter and the calibration parameter for the probability of detection of the co-existing signals, respectively. Thus, based on the processing scheme of Fig. 4, the complexity of RSFT-based processing for slow-time and fast-time coding schemes are $O\left(\frac{T}{L}(UL + U\log R + \phi) + U\right)$ and $O\left(T(NR\log R + \phi) + U\right)$, respectively.

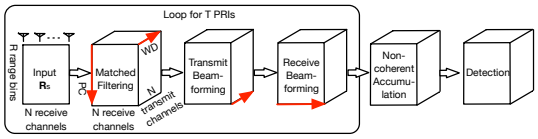

(a)

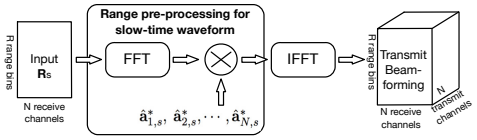

(b)

Fig. 3. **Conventional MIMO Radar Signal Processing for Fast-time Coded Waveforms.** (a) Overview of MIMO radar processing for fast-time coded waveforms. The matched filtering, transmit and receive beamforming are applied in each pulse. A non-coherent accumulation over T pulses is applied. (b) Matched filtering and range pre-processing for fast-time coded waveforms.

Remark 1. The computational savings of the slow-time coding scheme are not significant, mainly due to its WD, whose most computational intensive part cannot take advantage of the RSFT. On the other hand, since the fast-time coding scheme can use the RSFT in all stages, the corresponding reduction of complexity can be significant.

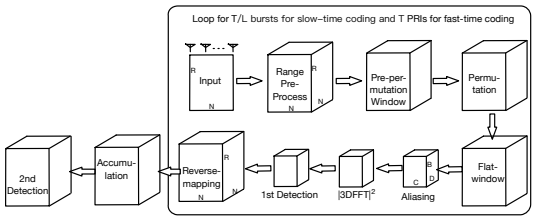

Fig. 4. **MIMO-RSFT Radar Signal Processing for Both Slow-time and Fast-time Coding Schemes.** In each iteration, the input for slow-time and fast-time coding is a burst of pulses and a single pulse, respectively.

C. The Asymptotically Optimal Detection Thresholds for MIMO-RSFT Radar

The derivation of the optimal thresholds for the two detection stages for the RSFT in the one-dimensional case can be found in [9]. Here, we derive the optimal thresholds for the MIMO-RSFT radar with fast-time coded waveforms by providing the key steps, which are unique for our problem. The derivation is based on hypothesis test on each resolution cell in the two detection stages of the RSFT, and the optimal thresholds are sought to minimize the worst case signal SNR for a given detection specification.

Let us consider the received signal from the i_{th} element with the model of (1). After the range pre-processing, the signal

output from the u_{th} matched filter is

$$\begin{aligned}\mathbf{m}_{i,u} &= \mathbf{H}_u \mathbf{D}\mathbf{r}_i \\ &\approx e^{ji\pi \sin\theta_k} \sum_{k\in[K]} \left(b_k \mathbf{A}_u \mathbf{v}(\omega_{t_k}) e^{ju\pi\sin\theta_k}\right) + \mathbf{H}_u \mathbf{D}\mathbf{n},\end{aligned} \tag{5}$$

where $\mathbf{H}_u = \text{diag}(\hat{\mathbf{a}}_u^*)$; $\mathbf{D}$ is the DFT matrix; $\mathbf{A}_u = \text{diag}(|\hat{\mathbf{a}}_u|^2)$; $\mathbf{v}(\omega_{t_k})$ is a complex sinusoid whose frequency is ω_{t_k}, which is related to the time delay (range) of the k_{th} target. Specifically, $\omega_{t_k} = t_k \Delta\omega_R, \Delta\omega_R = 2\pi/R$, and $\mathbf{v}(\omega_{t_k}) = [1,\ e^{-j\omega_{t_k}}, \cdots, e^{-j(R-1)\omega_{t_k}}]^T$.

Remark 2. After the range pre-processing, the signal part along the range dimension becomes a superposition of K sinusoids, whose frequencies are determined by the time delay of each target, and their amplitudes are modulated by the baseband signals' power spectrum. Moreover, (5) is similar to the signal model in [9], and $\mathbf{A}_u$ can be viewed as the pre-permutation window that is applied on the signal in the range dimension.

Based on Remark 2, the following derivation follows the same steps as in [9]. More specifically, let us denote the data cube after the 3-D FFT in the reduced space by $\hat{\mathbf{F}} \in \mathbb{C}^{B\times C\times D}$, where B, C, D are the data lengths in each reduced dimension; each entry in $\hat{\mathbf{F}}$ is a circularly symmetric Gaussian variable, i.e., $[\hat{\mathbf{F}}]_{p,w,v} \sim \mathcal{CN}(0, \sigma^2_{p,w,v}), p \in [B], w \in [C], v \in [D]$. The variance $\sigma^2_{p,w,v}$ depends on whether the $(p,w,v)_{\text{th}}$ cell contains (at least) a significant frequency. Under the alternative hypothesis in the first stage of detection, $[\hat{\mathbf{F}}]_{p,w,v}$ contains at least the significant frequency corresponding to the weakest target, i.e., the m_{th} target. Then, under the assumption that the side-lobes (leakage) in all dimensions are far below the noise level, we have $\sigma^2_{p,w,v} \approx \sigma^2_{bm}\alpha + \sigma^2_n\beta$. On the other hand, under the null hypothesis, there is no significant frequency mapping to the $(p,w,v)_{\text{th}}$ cell, then, $\sigma^2_{p,w,v} \approx \sigma^2_n\beta$, and

$$\begin{aligned}&\alpha = \alpha_r\alpha_T\alpha_R, \quad \beta = \beta_r\beta_T\beta_R, \\ &\alpha_r = |\frac{1}{R}\mathbf{v}^T(\omega_p)\mathbf{V}_r\mathbf{v}(\omega_{t_m})|^2, \ \ \alpha_T = |\mathbf{v}^H(\omega_w)\mathbf{V}_T\mathbf{v}(\omega_{\theta_m})|^2, \\ &\alpha_R = |\mathbf{v}^H(\omega_v)\mathbf{V}_R\mathbf{v}(\omega_{\theta_m})|^2, \ \beta_r = \|\frac{1}{R}\overline{\mathbf{W}}_r\mathbf{P}_r(\sigma_s)\hat{\mathbf{a}}^*\|^2, \\ &\beta_T = \|\overline{\mathbf{W}}_T\mathbf{P}_T(\pi_s)\mathbf{w}_T\|^2, \ \ \beta_R = \|\overline{\mathbf{W}}_R\mathbf{P}_R(\delta_s)\mathbf{w}_R\|^2,\end{aligned} \tag{6}$$

where $\omega_p = p\frac{2\pi}{R}$, $\omega_w = w\frac{2\pi}{N}$, $\omega_v = v\frac{2\pi}{N}$, are the frequencies related to the $p_{\text{th}}, w_{\text{th}}, v_{\text{th}}$ row of each DFT matrix of the 3-D FFT, respectively; $\omega_{t_m} = t_m\Delta\omega_R$, $\omega_{\theta_m} = \pi\sin\theta_m$ are the frequencies produced by the time delay and the DOA of the m_{th} target. $\mathbf{V}_r = \sum_{i\in[R/B]} \overline{\mathbf{W}}_{ri}\mathbf{P}_r(\sigma_s)\mathbf{W}_r$; $\mathbf{V}_T = \sum_{i\in[N/C]} \overline{\mathbf{W}}_{Ti}\mathbf{P}_T(\pi_s)\mathbf{W}_T$; $\mathbf{V}_R = \sum_{i\in[N/D]} \overline{\mathbf{W}}_{Ri}\mathbf{P}_R(\delta_s)\mathbf{W}_R$, where $\mathbf{W}_r = \text{diag}(\hat{\mathbf{a}}^*)$, $\mathbf{W}_T = \text{diag}(\mathbf{w}_T)$, $\mathbf{W}_R = \text{diag}(\mathbf{w}_R)$, $\overline{\mathbf{W}}_r = \text{diag}(\overline{\mathbf{w}}_r)$, $\overline{\mathbf{W}}_T = \text{diag}(\overline{\mathbf{w}}_T)$, $\overline{\mathbf{W}}_R = \text{diag}(\overline{\mathbf{w}}_R)$, and $\hat{\mathbf{a}}^*$ is the conjugate of the averaged DFT of $\mathbf{a}_i, i \in [N]$; $\mathbf{w}_T, \mathbf{w}_R$ are the pre-permutation windows of the transmit and receive DOA dimension, respectively, while $\overline{\mathbf{w}}_r, \overline{\mathbf{w}}_T, \overline{\mathbf{w}}_R$ are the flat windows for each dimension. $\overline{\mathbf{W}}_{ri}, \overline{\mathbf{W}}_{Ti}, \overline{\mathbf{W}}_{Ri}$ is the i_{th} sub-matrix of $\overline{\mathbf{W}}_r, \overline{\mathbf{W}}_T, \overline{\mathbf{W}}_R$, which are comprised of the iB_{th} to the $((i+1)B-1)_{\text{th}}$ rows of $\overline{\mathbf{W}}_r$, iC_{th} to the $((i+1)C-1)_{\text{th}}$ rows of $\overline{\mathbf{W}}_T$, iD_{th} to the $((i+1)D-1)_{\text{th}}$ rows of $\overline{\mathbf{W}}_R$, respectively. $\mathbf{P}_r(\sigma_s), \mathbf{P}_T(\pi_s), \mathbf{P}_R(\delta_s)$ are permutation matrices, which are parametrized by the permutation parameters $\sigma_s, \pi_s, \delta_s$ for each dimension during the s_{th} PRI.

Remark 3. For the 3D-RSFT in MIMO-RSFT radar with signal model (1), the distributions of the signal in each resolution cell in the first stage of detection for both hypotheses have the same structure as in the 1-D case (see [9]), i.e., they are all zero-mean circularly symmetric Gaussian distributions. In the alternative hypothesis, the variance of the distribution is a weighted sum of the variance of the signal and noise. The weights, i.e., the α and β are the products of the weights from each dimension (see Eq. (6)).

Based on Remark 3, the following steps, which involve deriving the distributions in the second stage of detection and solving the optimization problem to find optimal thresholds, are the same as described in [9]. We omit the rest of the derivations due to lack of space.

D. Doppler Processing for the Fast-time Coded Waveform

The Doppler frequency adds an additional dimensionality in the processing. For fast-time coded waveform processing, The received signal $\mathbf{R}_s, s \in [T]$ are partitioned into T/P coherent processing intervals (CPIs), with each CPI contains P consecutive received data matrices. The Doppler processing, for example, the moving target detector (MTD) are applied on the same range, transmit DOA, receive DOA resolution cell within a CPI. In conventional processing, the MTD can be effectively implemented via FFT, hence including of MTD in the fast-time coded MIMO-RSFT radar is straightforward, i.e., the range pre-processing for each CPI generates a 4-D tensor of size $R \times N \times N \times P$, then the following 4-D RSFT procedures are carried out on such tensor.

V. Simulations

A. Targets Reconstruction

We verify the feasibility of MIMO-RSFT radar and compare to the FFT-based and SFT-based processing via simulation. The main parameters of the system are listed in Table I. We generate a signal from 4 targets according to (1). The parameters of targets can be arbitrarily chosen within the parameter space, which implies that the corresponding frequency components do not necessarily lie on the grid points. The targets' parameters used in the simulation are listed in Table II. Note that we set targets 3 and 4 being close to each other in range and DOA to test the resolution of the MIMO-RSFT radar.

In the 3-D RSFT and SFT processing, we choose $B = 128, C = 32, D = 32$, respectively. To apply the SFT for high dimensional data, we extend the SFT into high dimension with the techniques in [8]. The results are shown in Fig. 5. Comparing to the FFT-based processing, the 4 targets are reconstructed exactly via the RSFT-based processing, while the SFT-based method results in many false alarms due to the

TABLE I
SRUR PARAMETERS

Parameter	Symbol	Value
Number of range bins	R	1024
Number of antenna elements	N	128
Length of CDMA Code	M	256
Number of PRI	T	32
Wave length	λ	$0.03m$
Wave propagation speed	c	$3 \times 10^8 m/s$
PRI	T_p	$25.6ms$
Maximum range	R_{max}	$156.6km$
Sampling frequency (IQ)	f_s	$1MHz$

TABLE II
TARGET PARAMETERS

Target	Range (km)	DOA ($\circ$)	SNR (dB)
1	14.8	20	0
2	90	-28	-5
3	44.8	5	-10
4	45	8	-10

ineffective detection and the high side-lobes from the strongest target (Target 1) in the range and transmit DOA plane. Furthermore, compared to the conventional FFT-based processing, the resolution of the MIMO-RSFT does not degrade.

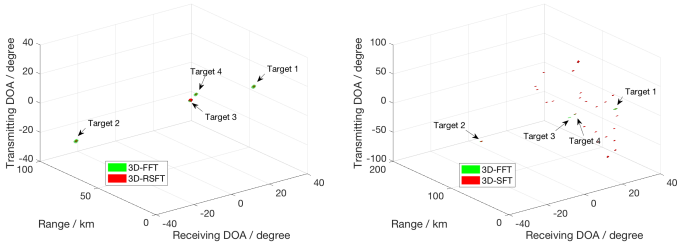

(a) (b)

Fig. 5. **Target Reconstruction via 3-D FFT, RSFT and SFT.** Comparing to the 3D-FFT, 3D-RSFT can recover the targets exactly, while the recovery via the 3D-SFT results into many false alarms due to the leakage from Target 1. (a) FFT vs RSFT. (b) FFT vs SFT.

B. Computational Savings

We compare the computational savings obtained by the MIMO-RSFT with that of the FFT-based processing both for slow-time and fast-time coded waveforms. The complexity of both slow-time and fast-time coding schemes is affected by the number of samples in the reduced space, i.e., $V = BCD$ and the signal sparsity K. A smaller V and K will lead to more computational savings of the MIMO-RSFT radar. For the slow-time coding scheme, Fig. 6 (a) shows that the RSFT-based processing does not save much even when V is small, and when V becomes larger, its complexity is even higher than that of the FFT-based processing. On the other hand, for the fast-time coding scheme, Fig. 6 (b) shows that the computational savings of the RSFT-based method is significant. We shall point out that since the RSFT trades off complexity and sensitivity, more savings in computation will result in a larger degradation of sensitivity [9], and the MIMO-RSFT radar offers an extra degree of freedom for designing a MIMO radar by trading off complexity with sensitivity.

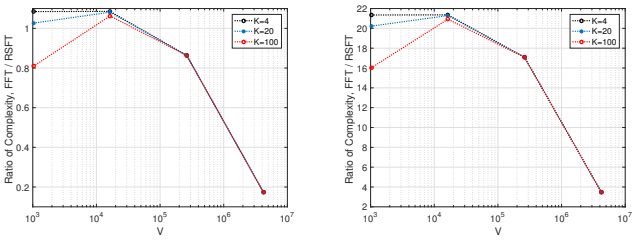

(a) (b)

Fig. 6. **Complexity Ration, FFT over RSFT.** $U = 2^{24}, V = \{2^{10}, 2^{14}, 2^{18}, 2^{22}\}, \eta_m = 4, \eta_p = 1$. Other parameters are the same as in Table I. (a) slow-time coding. $L = N, T = 4L$. (b) fast-time coding.

VI. CONCLUSION

In this paper, we have addressed the problem of reducing the implementation complexity of MIMO radars. To this end, we have proposed the MIMO-RSFT radar, which utilizes the RSFT to reduce the cost of the DSP based on a MIMO radar that works in a pulse mode. The complexity reduction for both slow-time and fast-time coded waveforms have been investigated, from which we have pointed out that the fast-time coded waveforms result in higher savings. Finally, the key steps of deriving the optimal detection thresholds for the MIMO-RSFT radar with fast-time coded waveforms have been demonstrated.

REFERENCES

[1] D. J. Rabideau and P. A. Parker, "Ubiquitous MIMO multifunction digital array radar and the role of time-energy management in radar," tech. rep., DTIC Document, 2004.

[2] J. Li and P. Stoica, "MIMO radar with colocated antennas," *Signal Processing Magazine, IEEE*, vol. 24, no. 5, pp. 106–114, 2007.

[3] H. He, P. Stoica, and J. Li, "Designing unimodular sequence sets with good correlations—including an application to MIMO radar," *IEEE Transactions on Signal Processing*, vol. 57, no. 11, pp. 4391–4405, 2009.

[4] H. Sun, F. Brigui, and M. Lesturgie, "Analysis and comparison of MIMO radar waveforms," in *2014 International Radar Conference*, pp. 1–6, IEEE, 2014.

[5] K. Hamid and M. Viberg, "Two decades of array signal processing research," *IEEE signal processing magazine*, vol. 13, no. 4, pp. 67–94, 1996.

[6] M. A. Richards, *Fundamentals of radar signal processing*. Tata McGraw-Hill Education, 2005.

[7] H. Hassanieh, P. Indyk, D. Katabi, and E. Price, "Simple and practical algorithm for sparse Fourier transform," in *Proceedings of the Twenty-third Annual ACM-SIAM Symposium on Discrete Algorithms*, SODA '12, pp. 1183–1194, SIAM, 2012.

[8] S. Wang, V. M. Patel, and A. Petropulu, "Rsft: A realistic high dimensional sparse fourier transform and its application in radar signal processing," in *Military Communications Conference, MILCOM 2016-2016 IEEE*, pp. 888–893, IEEE, 2016.

[9] S. Wang, V. M. Patel, and A. Petropulu, "An efficient high-dimensional sparse Fourier transform," *ArXiv e-prints*, Oct. 2016.

[10] M. Skolnik, "Systems aspects of digital beam forming ubiquitous radar," tech. rep., DTIC Document, 2002.

[11] Y. Yu, A. P. Petropulu, and H. V. Poor, "MIMO radar using compressive sampling," *Selected Topics in Signal Processing, IEEE Journal of*, vol. 4, no. 1, pp. 146–163, 2010.

[12] S. Sun, W. U. Bajwa, and A. P. Petropulu, "MIMO-MC radar: A MIMO radar approach based on matrix completion," *IEEE Transactions on Aerospace and Electronic Systems*, vol. 51, no. 3, pp. 1839–1852, 2015.